

Using X-ray micro-tomography to probe microstructure and damage of structural materials

Henry Proudhon

Centre des Matériaux, MINES ParisTech, UMR CNRS 7633

WEMESURF contact course, Paris 21-25 juin



From Röntgen to CAT scans

It is a long way since Röntgen discovered X-rays in 1892. X-ray tomography has become very popular, first using synchrotron radiation and in medical scanners (CAT scans). Nowadays, X-ray lab tomography has become commercially available and allows to study almost all kind of materials...



Contents

1 X-Ray microtomography

- About X-Rays
- Principle of X-Ray microtomography
- Synchrotron radiation vs lab sources
- Other contrast mechanisms
- Sample environment for in situ testing

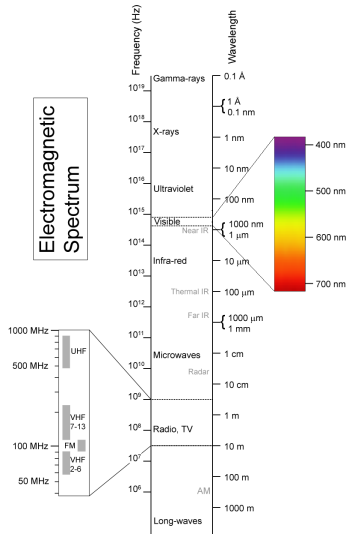
2 Applications

- Damage of polymer materials
- Observation of a fretting crack by X-ray tomography
- In situ study of fatigue crack propagation by XMT
- Fatigue cracking of β Ti alloy studied by DCT+XMT

3 Summary

X-rays

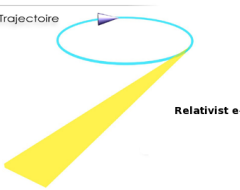
Electromagnetic Spectrum



Emission

X-rays are emitted by electron subjected to acceleration

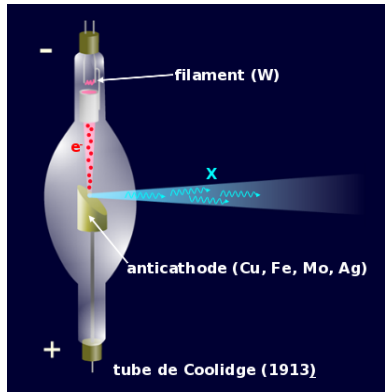
$$0.01 \text{ nm} < \lambda_X < 10 \text{ nm}$$



Synchrotron radiation



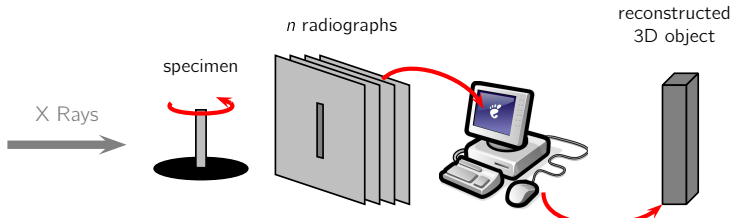
X-ray tube



X-ray tube

- vacuum tube that produces X-rays
- invented by William Coolidge in 1913
- used a lot for Medical Radiography
- electrons come from W cathode, are accelerated and then hit the anode
- a window allows for escape of the generated X-ray photons

Computed X-ray Micro-Tomography (XMT)



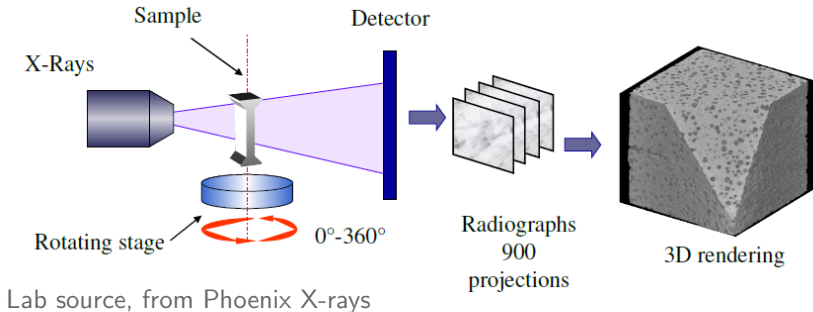
ESRF Grenoble



SR X-ray tomography

- parallel beam → no magnification
- Sample size limited by CCD size, typically 1 mm
- Monochromatic coherent beam (phase contrast)
- Low availability

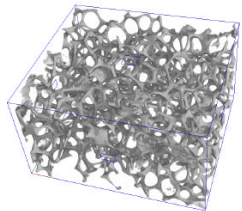
X-ray Micro-Tomography using a lab source



Lab source tomography

- Cone beam → magnification
- No monochromaticity
- High availability

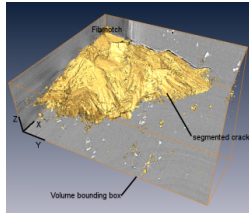
Some examples



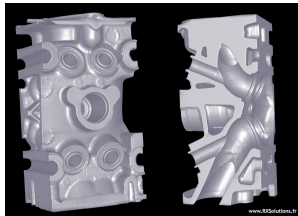
E. Maire, Al foam



P. Tafforeau, primate skulls



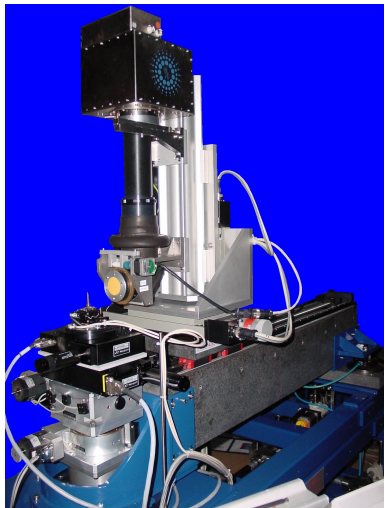
H. Proudhon, fatigue crack in Al alloy



culasse complète, RX solutions

Experimental setup at ID19

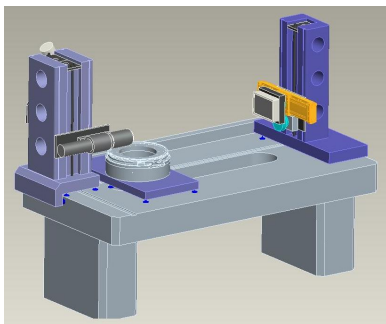
- Typical energy: 20 keV (5 to 90 keV)
- Long distance (145 m) → coherence (phase contrast)
- Multilayer monochromator: $\Delta\lambda/\lambda \simeq 10^{-2}$
- Inhouse Frelon CCD 14 bits camera $2048 \times 2048 \text{ px}^2$
- scan duration from 16 sec to several hours
- Sample environment: fatigue/tension machine, cold cell, furnace...



Contact: Elodie Boller (ESRF)

New tomographic setup available in F2M

- Full featured X-ray micro CT equipment
- Isotropic voxel size from $0.5 \mu\text{m}$ to $\simeq 100 \mu\text{m}$
- High mechanical stability (ability to receive *in situ* testing devices)
- Location: Institut Navier (Champs sur Marne)
- First images: Jan 2010



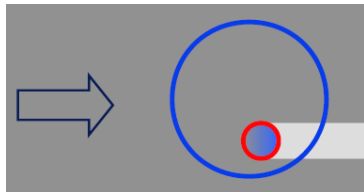
FÉDÉRATION
FRANCILIENNE
DE MÉCANIQUE



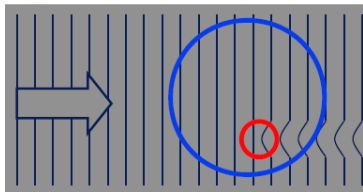
Matériaux • Structures • Procédés

Phase contrast imaging

Absorption



Phase



Main benefits

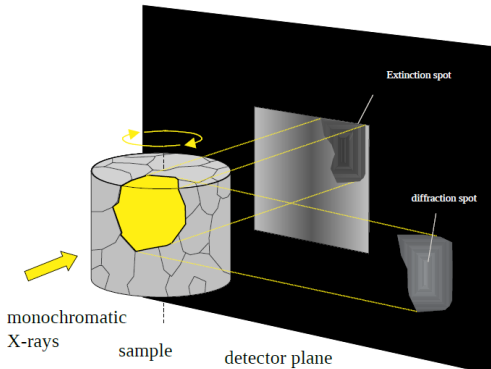
1 Improve sensitivity

Absorption contrast too low (improved spatial resolution, crack detection, similar attenuation)

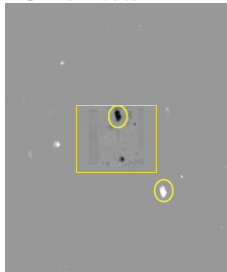
2 Reduce dose

Increase energy: Absorption \searrow replaced by phase contrast

Diffraction contrast tomography



DCT raw data:



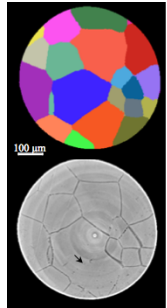
- Pixel size 2.4 μm
- ID11 (high flux)
- Sample with 1000 grains
→ ≈ 80000 diffraction spots
on 7200 images

DCT on Ti alloy

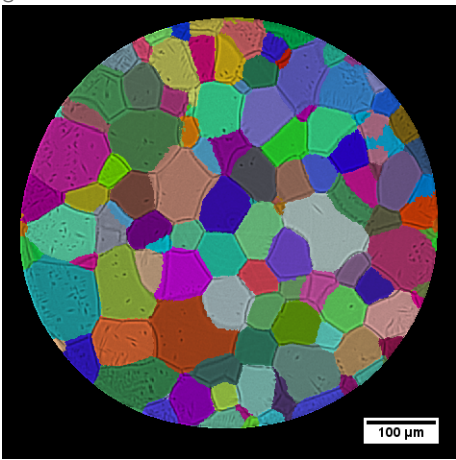
β -titanium alloy *Timet 21S*

Chemical composition:

15 wt% Mo, 3 wt% Nb



Heat treated sample + DCT reconstructed grains



Problem

in situ mechanical testing

- The load going through the specimen must be sustained by the *in situ* device
- A classical mechanical device: 2 columns and a crosshead
- X-ray tomography → rotation over 180 or 360°
- ⇒ no column allowed (many radiographs become unusable)



Solution

Axisymmetrical tube

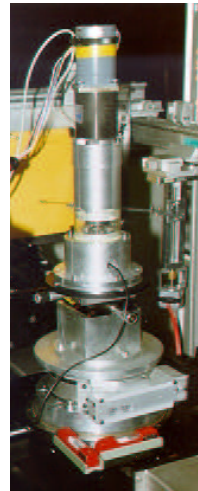
- Low X-ray absorption
- Uniform thickness
- Very good surface quality (polished)
- Load carrying capacity

Material candidates

PMMA, Polycarbonate, Al, Mg...

Tension Machine

- Stepper motor
- Force sensor 50 N to 5 kN
- Crosshead displacement monitored

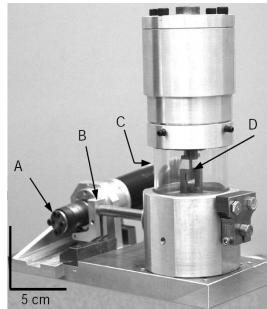


Buffière et al. Acta Mater 1998

Fatigue

In situ fatigue machine

- Electrical motor fitted with a crankshaft
- Force sensor 50 N to 5 kN
- High frequency ≤ 50 Hz



- A** Cam with elliptical cross section
- B** Eccentric moving the lower grip
- C** Transparent tube
- D** Specimen

[Buffière et al., 2006] Mat. Sci. Tech.

in situ tension at high temperature XMT

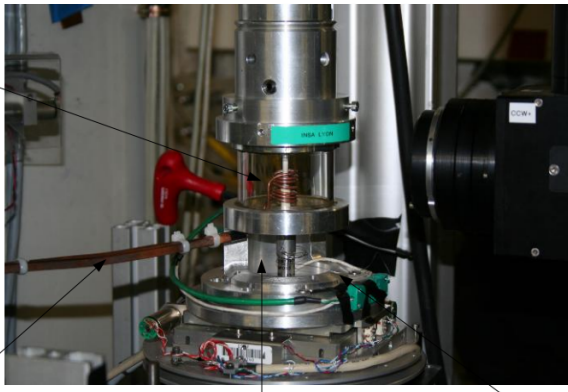
Bobine
d'induction

Détecteur

Câble rigide
d'alimentation

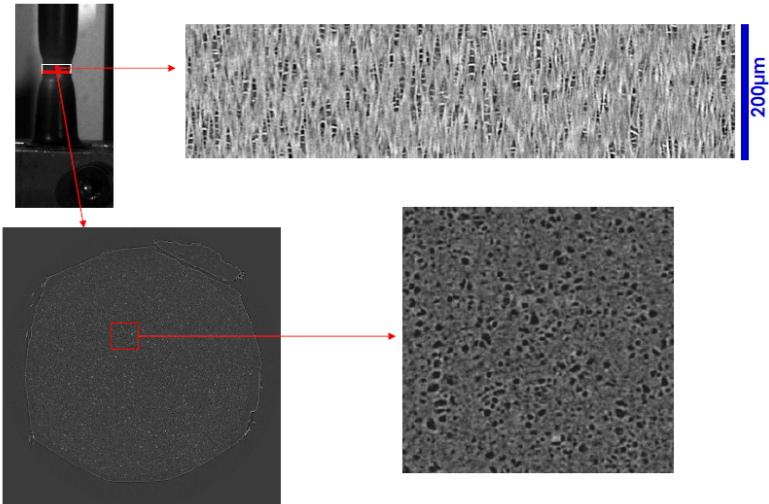
Câbles des
thermo-couples

Ouverture du bâti pour
permettre une rotation sur 180°



Suery & al, collab. SIMAP, LMS, MATEIS, ICMCB

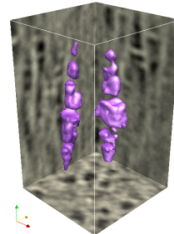
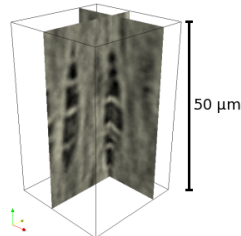
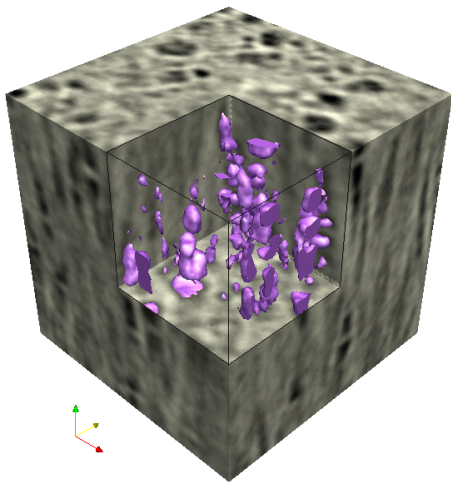
Necking and whitening of PA6



Necking

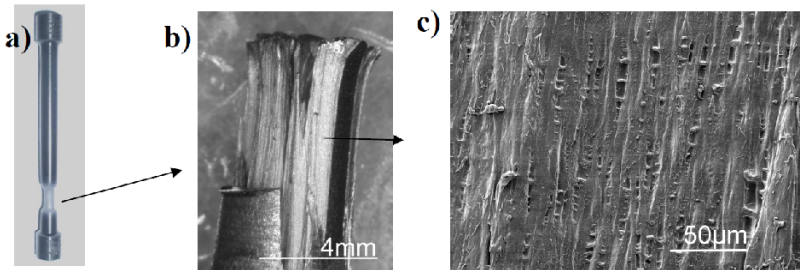
[Laiarinandrasana et al., 2010] J. of Polymer Sci. B

3D rendering of cavities observed after creep



[Laiarinandrasana et al., 2010] J. of Polymer Sci. B

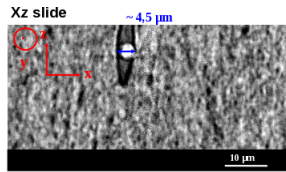
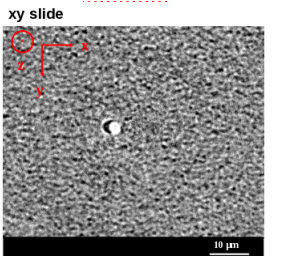
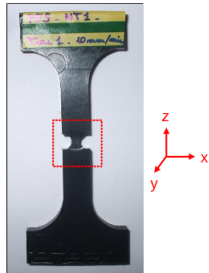
Cryofractography of PA6 sample



Cryofractography observation

- This confirms the X-ray microtomography observations of elongated sharp edged voids containing *walls* of intact matter
- More observations are under way with \neq stress triaxiality ratios

Cracking of Polyethylene



- 2.2% carbon black
- interrupted tests on notched samples
- local tomography
- voxel size = 0.35 μm

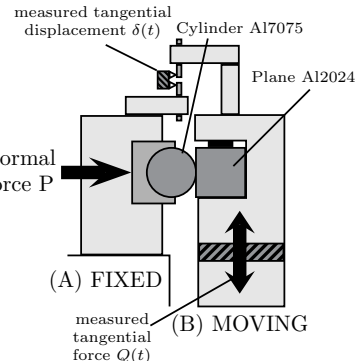
Two ≠ void populations

One very fine homogeneously distributed and one coming from particle decohesion

Experimental fretting tests

Fretting wear configuration

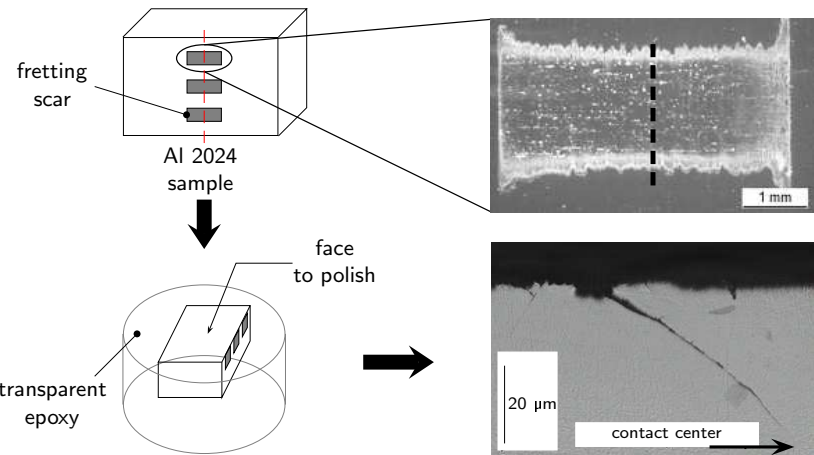
- Flat vs. Cylinder contact
- AA2024 damage tolerant aerospace alloy
- Partial slip condition
- Measure of P , $Q(t)$ and $\delta(t)$ during test
- number of cycles
 $0 < N \leq 4.10^6$



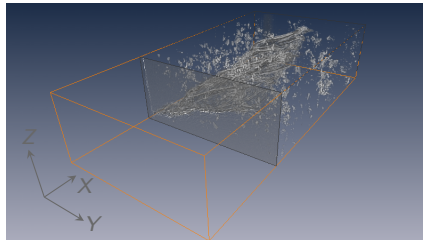
Fretting experiments were carried out at Ecole Centrale de Lyon



Fretting damage investigation

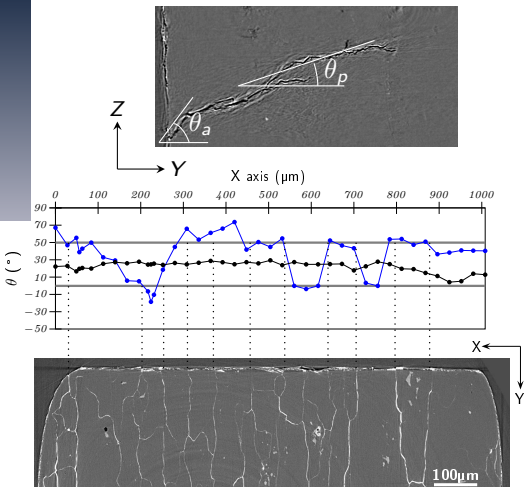


Study of a fretting crack by XMT¹



crack initiation angle θ_a

- 2 possible values:
0° or 45°
- strong correlation
with the GB
position



¹[Proudhon et al., 2007] Eng. Frac. Mech., vol. 74(5):782

Project aims

Experimental

Tomographic imaging for detailed insight of small crack evolutions (up to ~ 2 mm)

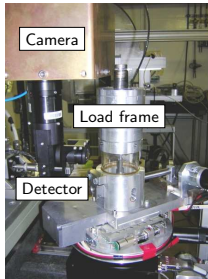
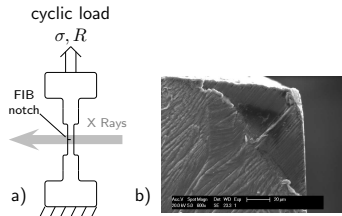
- Model alloy with ideally flat shape cracks
- Engineering 2027 alloy with highly complex crack shapes

Propagation model

Apply multi-mechanistic crack closure modelling to small corner cracks

- RICC and PICC
- Constant amplitude, constant ΔK and overload regimes
- Plane stress, plane strain and mixed stress state effects

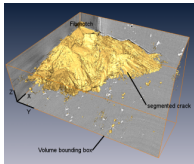
in situ X-ray tomography setup



in situ crack monitoring

- Two \neq alloys: 5091 (grain size $\sim 1 \mu\text{m}$) vs. 2027 (grain size $\sim 100 \mu\text{m}$)
- crack initiation is controlled via a FIB notch
- *in situ* fatigue device
- study both baseline growth ($\Delta K \sim 3 \text{ MPa}\sqrt{\text{m}}$) and post-overload growth

Tomographic data analysis



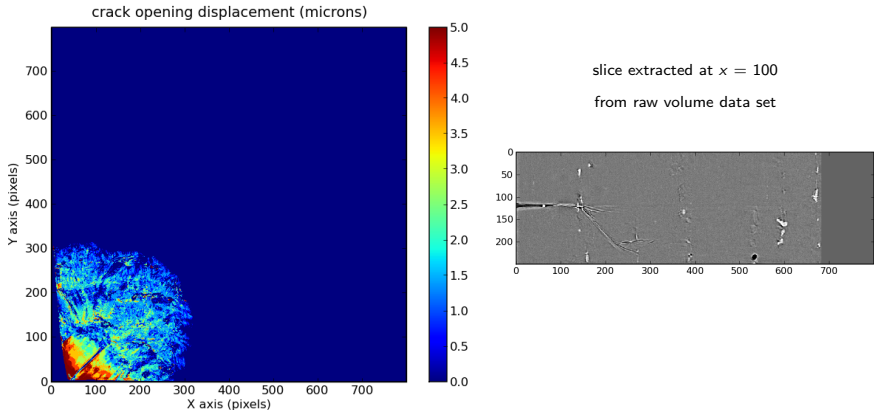
Amount of data is considerable (more than 100 scans) → need automated data treatment as *much as possible*...

For each tomographic image (x,y,z):

- crack front location and local da/dN values
- local crack opening values
- 3D rendering of crack morphology

Crack opening displacement in 2027

N=853k cycles + 100% OL + 59k cycles

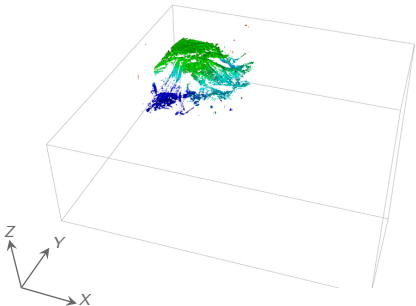


3D crack rendering in 2027

N=853k cycles + 100% OL + 59k cycles

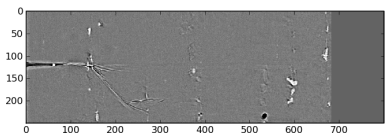
3d rendering with position mapping

box is $(560 \times 560 \times 175 \mu\text{m})$

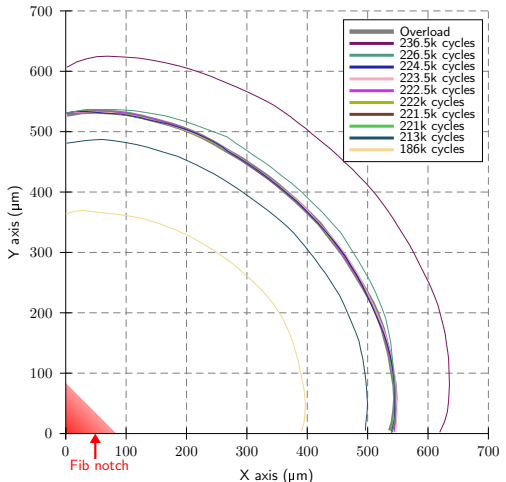


slice extracted at $x = 100$

from raw volume data set



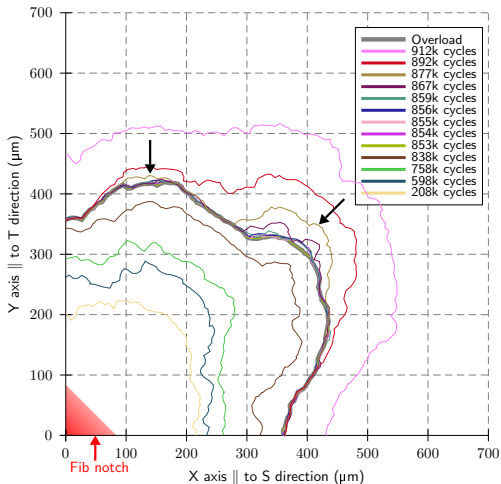
5091 vs. 2027 growth behavior



5091 crack growth

- Highly planar
- Microstructure independent
- Tunnelling 2-3%
- Overload stopped the crack, growth resumes from the bulk

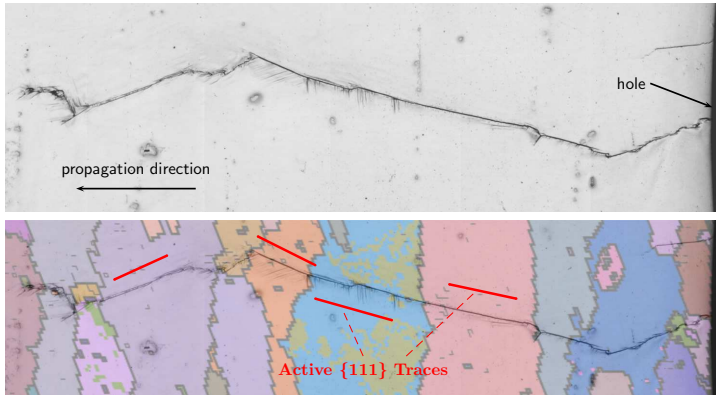
5091 vs. 2027 growth behavior



2027 crack growth

- Tortuous crack path
- Strongly microstructure dependent
- Multiple crack branching
- Tunnelling more pronounced
- Overload stopped the crack longer than in 5091, growth resumes from the bulk also

Surface analysis by EBSD



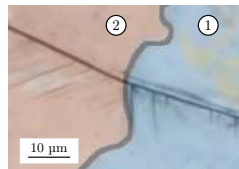
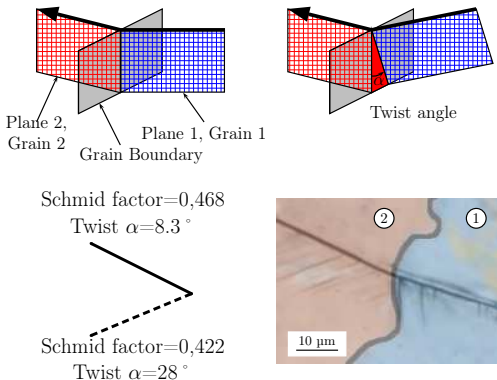
Highlight

The crack path seems to be well correlated to some of the {111} planes of the crossed grains...

Crack propagation mechanisms

Propagation mechanisms

- 1 propagation along $\{111\}$ planes
- 2 calculation of the active plane by Schmid factor
- 3 grain boundary crossing by minimising the twist angle



Summary

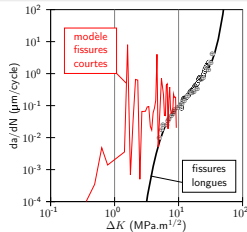
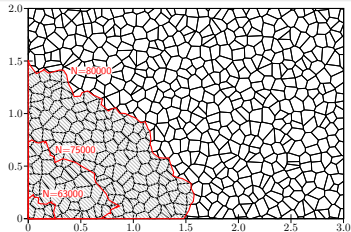
Correlation of cracking planes and twist angle mechanisms in 60% of the studied grains by EBSD ($\simeq 100$ grains).

Crystallographic Model overview

Model overview

Simple geometric model to account for the variability due to crystallographic orientations of the grains crossed by the crack

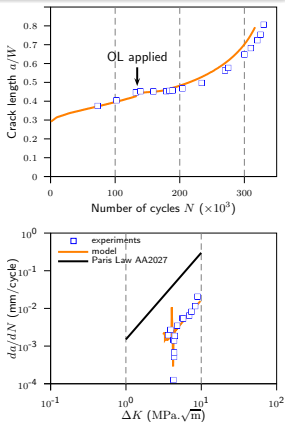
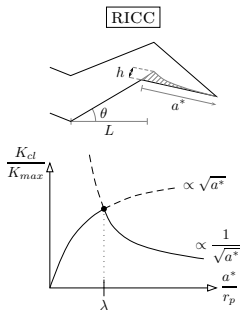
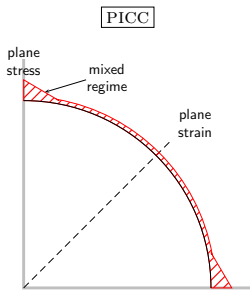
- 2D voronoi microstructure
- propagation allong most favoured $\langle 111 \rangle$ slip plane
- tilt and twist angle influence
- equivalent area K solution to determine crack growth rate



Southampton Model overview (I. Sinclair)

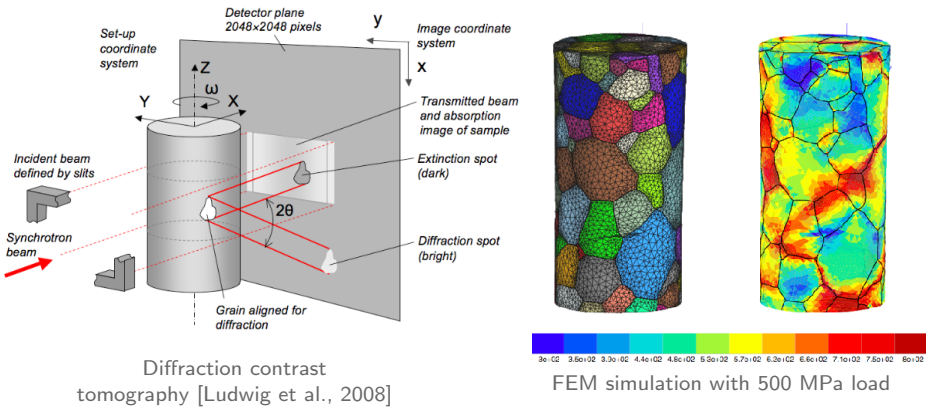
Extended multi-mechanistic crack closure model

Apply to both CA growth and post-overload growth with mixed regime plane stress/plane strain description



Imaging grains in 3D with tomography

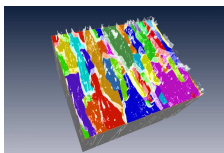
- French ANR project CRYSTAL (starting end of 2010)
- partners: Mines ParisTech, INSA Lyon, Onera



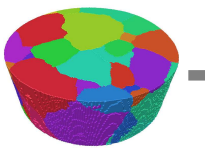
Simulation 3D de la microstructure

- 1** Couplage avec la caractérisation 3D pour la simulation de microstructures réelles

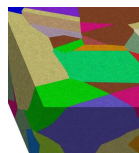
Gallium + XMT
+ EBSD



grain tracking
(W. Ludwig)

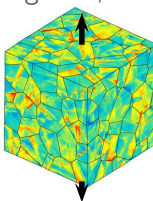
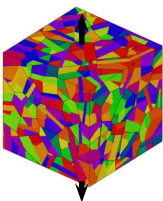


maillage de la micro-
structure réelle



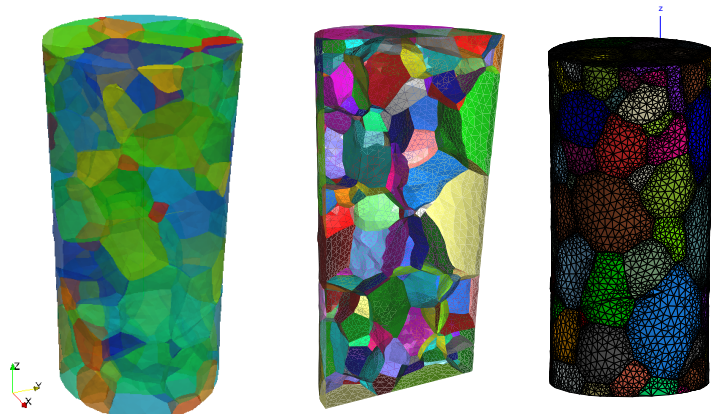
- 2** Microstructures numériques pour étudier l'influence des paramètres : taille et forme des grains, texture...

agrégat polycristallin
bainite, 120 grains
Centre des Matériaux
Mines Paris



contrainte locale
dans l'agrégat

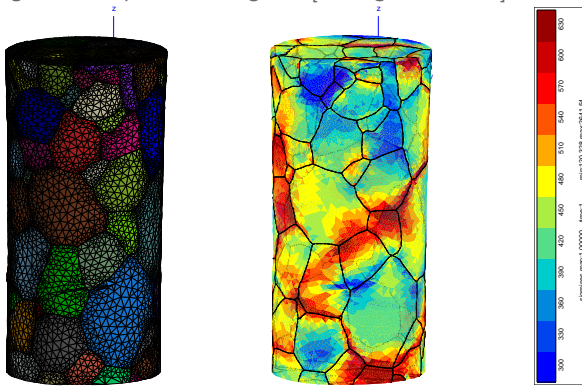
Numerical avatar of Ti specimen



- Grains from DCT experiment
- Grain boundaries meshed with shell elements (only half of the sample is shown)
- Full 3D mesh ready for Finite Elements computation

Computation under tension

mesh from DCT image of ti sample with 130 grains [Ludwig et al., 2009]:



Current focus

Introducing cracks within the mesh to compare to experimental crack propagation observed by 3D XMT

Summary

Computed X-ray microtomography is a powerful tool to investigate damage and microstructure organisation within a wide range of materials

Key figures using synchrotron radiation

- Resolution down to $0.12 \mu\text{m}$ ($0.7 \mu\text{m}$ is routine at ID19, ESRF)
- Phase, absorption and diffraction contrasts
- *in situ* experiments

Lab tomography more and more available

- complementary of SR X-ray tomography with **higher availability**
- similar capabilities in many cases but not always...

-  Buffière, J., Ferrié, E., Proudhon, H., and Ludwig, W. (2006).
3D visualisation of fatigue cracks in metals using high resolution synchrotron.
Material Science and Technology, 22(9):1019–1024.
-  Laiarinandrasana, L., Morgeneyer, T. F., Proudhon, H., and Regrain, C. (2010).
Damage of semicrystalline polyamide 6 assessed by 3d x-ray tomography: From microstructural evolution to constitutive modeling.
Journal of Polymer Science Part B: Polymer Physics, 48(13):1516–1525.
-  Ludwig, W., King, A., Reischig, P., Herbig, M., Lauridsen, E., Schmidt, S., Proudhon, H., Forest, S., Cloetens, P., du Roscoat, S. R., Buffière, J., Marrow, T., and Poulsen, H. (2009).
New opportunities for 3d materials science of polycrystalline materials at the micrometre lengthscale by combined use of x-ray diffraction and x-ray imaging.
Materials Science and Engineering: A, 524(1-2):69–76.
Special Topic Section: Probing strains and Dislocation Gradients with diffraction.
-  Ludwig, W., Schmidt, S., Lauridsen, E. M., and Poulsen, H. F. (2008).
X-ray diffraction contrast tomography: a novel technique for three-dimensional grain mapping of polycrystals. I. Direct beam case.
Journal of Applied Crystallography, 41(2):302–309.
-  Proudhon, H., Buffière, J.-Y., and Fouvry, S. (2007).

Three dimensional study of a fretting crack using synchrotron X-ray microtomography.

Engineering Fracture Mechanics, 74(5):782–793.